



DOI: 10.46793/41DAS2025.111P

QUASI-STATIC AND DYNAMIC BEHAVIOR OF VANADIUM-CARBIDE REINFORCED ALUMINUM ALLOY STUDIED VIA DIGITAL IMAGE CORRELATION – PRELIMINARY STUDY

Miloš PEŠIĆ¹, Aleksandar BODIĆ², Marko TOPALOVIĆ³, Snežana VULOVIĆ⁴, Vladimir DUNIĆ⁵, Vladimir MILOVANOVIĆ⁶, Miroslav ŽIVKOVIĆ⁷

- ¹ <u>0000-0002-3405-5216</u>, Institute for Information Technologies, Jovana Cvijića bb, Kragujevac, Serbia, E-mail: milospesic@uni.kg.ac.rs
 - ² 0000-0002-1713-6540, Faculty of Engineering, Sestre Janjić 6, Kragujevac, Serbia, E-mail: abodic@uni.kg.ac.rs
- 0000-0001-6101-755X, Institute for Information Technologies, Jovana Cvijića bb, Kragujevac, Serbia, E-mail: topalovic@kg.ac.rs
- ⁴ <u>0000-0001-5784-0906</u>, Institute for Information Technologies, Jovana Cvijića bb, Kragujevac, Serbia, E-mail: vsneza@kg.ac.rs
- ⁵ 0000-0003-1648-1745, Faculty of Engineering, Sestre Janjić 6, Kragujevac, Serbia, E-mail: dunic@kg.ac.rs
- 6 0000-0003-3071-4728, Faculty of Engineering, Sestre Janjić 6, Kragujevac, Serbia, E-mail: vladicka@kg.ac.rs
- O000-0002-0752-6289, Faculty of Engineering, Sestre Janjić 6, Kragujevac, Serbia, E-mail: miroslav.zivkovic@kg.ac.rs

1. Introduction

Vanadium-carbide reinforced aluminum alloys have attracted significant interest in recent years due to their enhanced strength-to-weight ratio, improved fatigue resistance, and refined microstructural stability, making them promising materials for lightweight protective structures and high-performance engineering applications [1, 2, 3]. The addition of vanadium carbide promotes grain refinement and precipitation strengthening, which can substantially improve mechanical performance under different loading regimes.

The mechanical response of aluminum alloys is strongly dependent on the strain rate, with dynamic loading often leading to increased flow stress and reduced ductility compared to quasi-static conditions [4]. Investigations of aluminum alloys such as 6005A-T6 and 5083 have shown that these materials exhibit notable strain rate sensitivity, which must be taken into account in structural design and numerical modeling.

Full-field optical measurement techniques, particularly Digital Image Correlation (DIC), have become indispensable in characterizing strain localization and deformation behavior in both quasi-static and high-strain-rate testing. Ultra-high-speed DIC has been successfully applied to capture

deformation fields during impact events such as Taylor impact tests, providing detailed insight into localized plasticity and failure mechanisms [2, 3]. Moreover, DIC has been extensively used to assess the formability of aluminum alloys and to study crack initiation and propagation under various loading conditions, offering valuable data for fracture mechanics and forming limit analyses [5].

In this study, quasi-static and dynamic tensile testing of a vanadium-carbide reinforced aluminum alloy is presented, with full-field strain measurements obtained using Digital Image Correlation. The objective is to evaluate the influence of strain rate on mechanical behavior, visualize strain distribution during deformation, and provide experimental data for the future validation of computational models.

2. Materials and Methods

An Al–VC surface-reinforced layer was produced by laser surface alloying. Commercial VC powder was uniformly spread on an aluminum plate, and the surface was scanned in multiple laser passes, melting the Al surface and mixing VC into the melt pool. Alternating scan directions promoted homogenization; inert shielding and gentle post-cleaning removed loose residue.







Tensile flat dog-bone specimens were extracted so that the laser-alloyed zone spans the gauge. The same specimen design was used in both quasi-static and dynamic tests to enable direct rate comparisons. Surfaces in the gauge were lightly finished and coated with a matte white base plus a fine black speckle for DIC, as shown in Fig.1.



Fig. 1. Flat dog-bone tensile specimen with central neck prepared for testing; DIC grid applied over the gauge region

Quasi-static tensile tests were conducted on a universal Instron machine in displacement control at 0.001 mm/min under laboratory conditions. Force and crosshead displacement were recorded and time-aligned with imaging. Five tests were conducted to check repeatability.

Dynamic tensile tests were performed on a tensile SHB configuration targeting an average strain rate of $\sim 1000~\text{s}^{-1}$. Incident, reflected, and transmitted bar strains were measured with axial gauges and reduced using standard one-dimensional elastic-wave analysis. Stress equilibrium was verified by comparing $\sigma_{\text{inc}} + \sigma_{\text{ref}}$ with σ_{trans} over the analysis window.

Full-field strain was measured with MatchID software.

- QS: monochrome industrial camera with a macro lens and symmetric continuous LED lighting.
- SHB: high-speed camera with short exposure, hardware-synchronized to the SHB DAQ.

Calibration and correlation parameters (subset/step) were kept consistent within each regime and chosen based on speckle size. Axial strain was obtained from a virtual extensometer in the gauge.

For QS, engineering stress-strain curves were built from measured force and initial area with DIC-based axial strain; the yield strength was determined by the 0.2% offset method. For SHB, true stress-strain was derived from bar signals. Strain-rate sensitivity was quantified by comparing flow stress

at matched plastic strain levels; DIC major-strain maps supported the discussion of localization and failure mode.

3. Experimental setup

Material fabrication. The Al–VC surface-reinforced layer was produced by laser surface alloying: VC powder was uniformly spread on an Al plate, then multiple laser passes melted the surface and mixed VC into the melt pool, forming a continuous composite layer upon solidification. Cross-sections were prepared separately to confirm layer continuity and thickness.

Specimens and fixtures (common to both regimes). Flat dog-bone specimens were extracted so that the laser-alloyed zone spans the gauge. Custom pin-loaded fixtures engaged the holes to avoid grip-induced damage and to ensure repeatable alignment. Gauge surfaces were finished and speckled for DIC.

Quasi-static tensile setup. Tests were run on a universal Instron frame in displacement control (0.001 mm/min) under laboratory conditions, as shown in Fig.2. Force and crosshead displacement were recorded and time-aligned with imaging; duplicate tests were performed to check consistency.

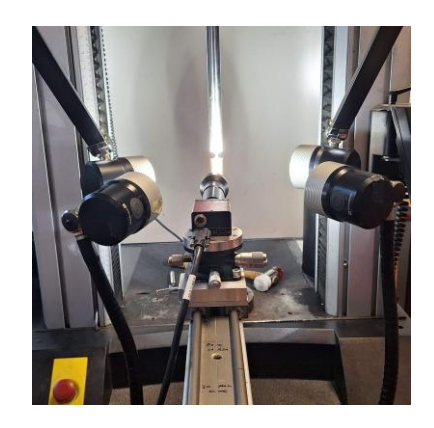


Fig. 2. DIC arrangement with four continuous LED lights providing symmetric illumination of the gauge region

Dynamic tensile (Split-Hopkinson Bar) setup.

Dynamic tests used a tensile SHB configuration with adapters that pin-loaded the same flat specimen design, as shown in Fig.3. Axial strain gauges on the incident and transmitter bars recorded incident, reflected, and transmitted waves. Classical one-dimensional elastic-wave analysis was used to obtain specimen stress, strain, and strain-rate; stress equilibrium was checked by comparing $\sigma_{\rm inc}+\sigma_{\rm ref}$







with σ_{trans} over the analysis window. Tests targeted an average strain rate of ~1000 s⁻¹.

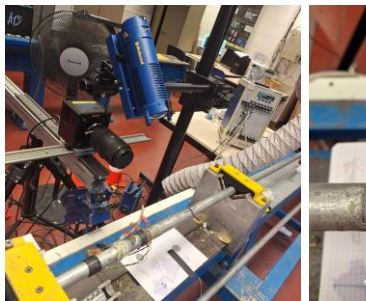




Fig.3. Tensile Split-Hopkinson Bar (SHB) setup: overall arrangement with high-speed camera and lighting - left; close-up of the flat dog-bone specimen mounted between the SHB tensile adapters - right

Digital Image Correlation and timing. DIC was performed in the MatchID software for both regimes. For QS, a monochrome industrial camera with a macro lens and continuous symmetric LED lighting was used. For SHB, a high-speed camera with short exposure was hardware-triggered from the SHB acquisition to ensure frame-accurate synchronization. Calibration and correlation parameters were kept consistent within each regime; axial strain was taken from a virtual extensometer along the gauge.

Data reduction and comparison metric. QS engineering curves were built from measured force and initial area with DIC-based axial strain. SHB analysis yielded true stress—strain. Strain-rate sensitivity was assessed by comparing flow stress at matched plastic strain levels; DIC maps were used to discuss strain localization and failure mode under the two loading rates.

4. Results and Discussion

4.1 Quasi-static stress-strain comparison (Al vs. Al-VC)

Fig. 4 compares the engineering stress–strain responses of the unreinforced aluminum (Al) and the laser-alloyed Al–VC test specimen tested under identical conditions. Both materials show a steep elastic segment with a similar initial slope, followed by measurable hardening and a smooth transition to localization. The Al–VC curve exhibits a higher proof/peak stress in the early plastic range, by roughly one order of 10% relative to Al, consistent with particle strengthening of the laser-alloyed layer.

Beyond approximately $\epsilon \sim 0.30-0.35$, the curves converge and then cross: the unreinforced Al

maintains slightly higher flow stress and continues to larger terminal strain, whereas Al–VC softens earlier and fractures at a somewhat lower global strain. This behavior indicates that while VC reinforcement raises initial strength, it also reduces the available work-hardening/ductility, leading to earlier localization – a trend corroborated by the DIC fields presented later.

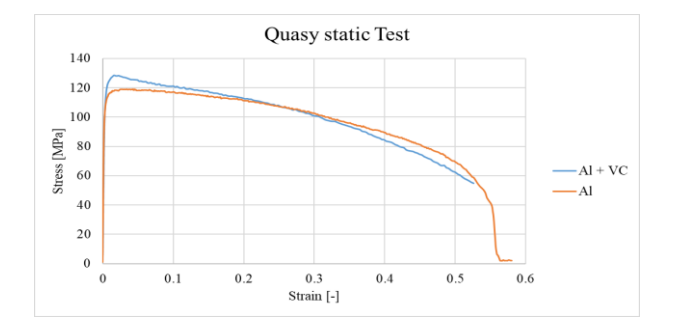


Fig. 4. Quasi-static engineering stress–strain curves of Al and Al–VC flat coupons – identical geometry and test conditions

Strain is obtained from a DIC virtual extensometer. Al–VC test specimen shows higher early strength (~8–10% above Al), whereas at larger strains the unreinforced Al carries slightly higher stress and reaches a larger terminal strain.

Fig.5 shows representative major-strain maps recorded by the camera for the Al-VC test specimen. The field is uniform at the start, a faint axial band appears with the onset of plasticity, and the band progressively intensifies and narrows near peak load, culminating in a sharply confined neck in the last frame. All frames are plotted with the same color scale and field of view to allow direct visual comparison.

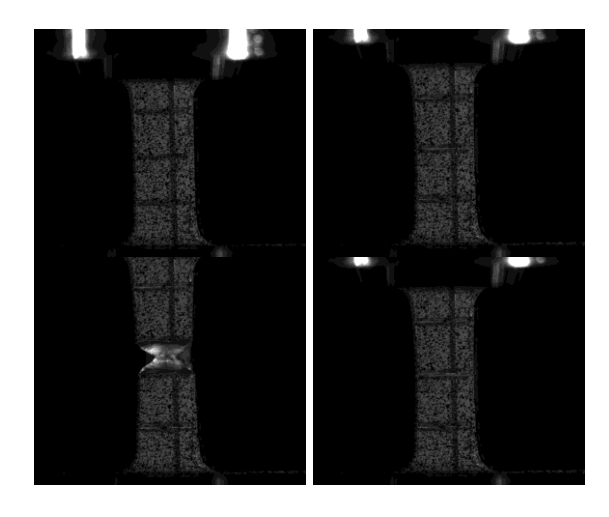


Fig.5. DIC major-strain fields (Al-VC test specimen): baseline → band nucleation → localization growth → fracture (clockwise)







4.2 Dynamic vs. quasi-static tensile response (Al–VC)

Fig. 6 compares quasi-static and dynamic responses of the Al–VC test specimens. After a brief transient, the dynamic curve stays approximately 20% higher in early plasticity and remains elevated while softening to a larger terminal strain – evidence of strain-rate strengthening with rate-dependent hardening tempered by progressive softening (e.g., adiabatic heating) as localization develops.

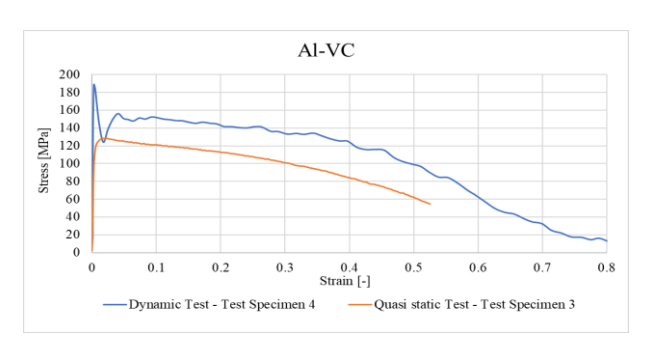


Fig. 6. Engineering stress–strain curves for the Al–VC flat test specimens under quasi-static and dynamic loading (identical geometry).

The dynamic curve shows an initial transient followed by a stable, higher flow level and a larger terminal strain than the quasi-static response.

Fig. 7 shows representative dynamic-test majorstrain maps: an initially uniform field evolves into a central axial band that tightens into a narrow localization zone. In the last frame, the peak strain is strongly confined to the neck with steep lateral gradients, consistent with the gradual post-peak softening of the dynamic curve and the extended global strain to failure.

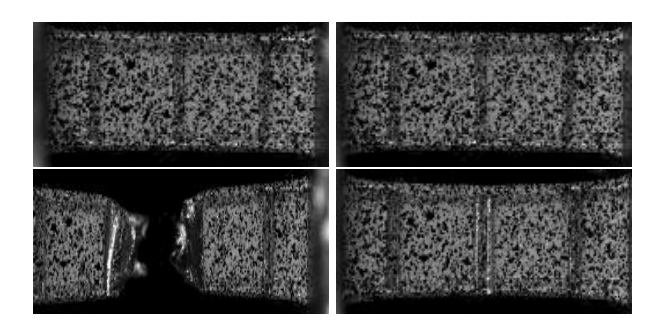


Fig. 7. Dynamic (SHB) DIC major-strain fields for Al– VC at four stages: baseline → band nucleation → localization growth → fracture (clockwise)

The curves and DIC fields show that Al-VC exhibits rate-dependent strengthening and sharper, more confined localization under dynamic loading compared with the quasi-static case. For concise

quantification, the study reports classic strength values (0.2% proof, UTS) and two field-aware indicators: the global strain at localization onset and the peak local major strain before fracture, extracted consistently from the DIC analysis for each regime.

5. Conclusions

Quasi-static and dynamic tests on the laser alloyed Al–VC test specimens show a clean, repeatable tensile response: DIC captures the evolution from near-uniform straining to a single, gauge-centered neck, while dynamic loading sustains higher flow stress over a wide strain range and culminates in a sharper, more confined localization than the quasi-static case – establishing a concise, rate-dependent baseline and field-level validation targets for modeling.

For future work, complementary fractography and coupled thermo-mechanical simulations will be done to link microstructure to localization.

Acknowledgement

This research is partly supported by the Science Fund of the Republic of Serbia, #GRANT No 7475, Prediction of damage evolution in engineering structures – PROMINENT, and by the Ministry of Science, Technological Development and Innovation, Republic of Serbia, Agreement No. 451-03-136/2025-03/200378 and Agreement No. 451-03-137/2025-03/200107.

References

- [1] D. Erdeniz, W. Nasim, J. Malik, *et al.* Effect of vanadium micro-alloying on the microstructural evolution and creep behavior of Al-Er-Sc-Zr-Si alloys. *Acta Materialia*, 2017, 124, 501–512. DOI: 10.1016/j.actamat.2016.11.033.
- [2] X. Chen, J. Chen, W. Xi, *et al.* Effect of Vanadium Addition on Solidification Microstructure and Mechanical Properties of Al–4Ni Alloy. *Materials*, 2024, 17(2), 332. DOI: 10.3390/ma17020332.
- [3] A. Kumar, C. Sasikumar. Effect of Vanadium addition to Al–Si alloy on its mechanical, tribological, and microstructure properties. *Materials Today: Proceedings*, 2017, 4, 10768–10772. DOI: 10.1016/j.matpr.2017.01.026.
- [4] A. S. Khan, H. Liu. Variable strain rate sensitivity in an aluminum alloy: Response and constitutive modeling. *International Journal of Plasticity*, 2012, 36, 1–14. DOI: 10.1016/j.ijplas.2012.02.001.
- [5] R. P. Bigger, A. Carpenter, N. Scott, et al. Dynamic Response of Aluminum 5083 During Taylor Impact Using Digital Image Correlation. Experimental Mechanics, 2018, 58(6), 913–923. DOI: 10.1007/s11340-018-0392-5.